JOURNAL OF AGRICULTURAL AND FOOD CHEMISTRY

pubs.acs.org/JAFC Article

Synergistic Activation of Immune Pathways by Pesticide Chlorpyrifos and Its Metabolite 3,5,6-Trichloro-2-Pyridinol Mixtures in Fish

Huo-Bin Tang, Jun-Hao Chen, Jian-Rao Hu,* and Hong-Liang Lu*

Cite This: J. Agric. Food Chem. 2026, 74, 16553−16562 Read Online

ACCESS | Metrics & More | Article Recommendations | Supporting Information

ABSTRACT: Various pesticides and their metabolites commonly co-occur in aquatic environments, yet their combined effects are often overlooked. In this study, alterations in blood physiology (e.g., routine blood parameters, erythrocyte damage, respiratory burst, serum metabolomics, and expression of immune- and inflammation-related genes) in crucian carp (*Carassius auratus*) following single and combined exposure to chlorpyrifos (CPF) and its metabolite 3,5,6-trichloro-2-pyridinol (TCP) were investigated. CPF mainly affected oxidative metabolism and immune activation, while TCP induced erythrocyte damage and hematological disorders. Notably, CPF + TCP coexposure markedly upregulated immune- and inflammation-related genes, activated toll-like receptors, and induced distinct hematological toxicity compared to single exposure. Coexposure triggered proinflammatory cytokines (e.g., *TNFα*, *IL-1β*, *IL-6*), and altered inflammation-related metabolites (e.g., prostaglandins, leukotrienes), forming a synergistic inflammatory cascade. These findings indicate that pesticide−metabolite mixtures synergistically activate innate immune pathways in aquatic organisms, offering insight into combined pesticide-metabolite toxicity in nontargeted aquatic species.

KEYWORDS: *Carassius auratus, inflammation, hematological toxicity, synergistic effects*

1. INTRODUCTION

Organophosphorus pesticides are among the most universally used agricultural chemicals globally, accounting for a high proportion due to their broad-spectrum insecticidal efficacy and relatively low persistence compared to organochlorine pesticides.[1] Chlorpyrifos [CPF, *O,O*-diethyl *O*-(3,5,6-trichloro-2-pyridyl) phosphorothioate] is an extensively used organophosphorus pesticide for pest control in agricultural and urban environments.[2] CPF can be environmentally degraded with a relatively long half-life (approximately 60 days), and 3,5,6-trichloro-2-pyridinol (TCP) is its primary intermediate metabolite in various environments.[3] Compared with CPF, TCP is more water-soluble and mobile, making it easier to release into aquatic environments.[3] Both of them have been frequently detected in surface waters, sediments, soils, as well as in biota near agricultural runoffs, raising concerns regarding their toxicological and ecological impacts.[4−6] In water bodies across different countries, CPF residual concentrations have exceeded allowable levels, even reaching up to 37.3 μg/L, a concentration far above the environmental limit,[7] while TCP often persists at similar or even higher levels due to its greater polarity and stability.[8]

As an organophosphorus pesticide, CPF exerts its primary toxic action by inhibiting acetylcholinesterase (AChE), leading to the accumulation of acetylcholine, thereby inducing neurotoxicity and finally resulting in the death of pests.[9] Besides the well-documented neurotoxic profile, CPF is also implicated in oxidative stress induction, immunomodulation, mitochondrial dysfunction, endocrine disruption, etc.[5,10−12] In contrast, despite lacking direct cholinesterase inhibition, TCP is not innocuous and has been documented to induce genotoxicity and endocrine activity in various aquatic organisms,[13,14] potentially implying differential toxicity mechanisms from CPF.

In fish, the innate immune system serves as the host's primary defense barrier against pathogens, and provides the essential foundation for the effective activation of adaptive immunity.[15,16] The crucian carp, *Carassius auratus*, is a widely distributed freshwater fish species and an ecologically relevant model for studying behavioral, physiological, and biochemical responses of aquatic organisms under environmental pollution due to its high sensitivity to pollutants and well-characterized immune and erythropoietic systems.[17,18] As a typical benthic fish, *C. auratus* is commonly exposed to sediment-bound and dissolved pollutants, and is ideally suited for the assessment of sublethal endpoints such as oxidative stress, immune function, and hematological parameters.[19−21] Prominent physiological and transcriptomic alterations in *C. auratus* upon exposure to various pollutants, including pesticide and pharmaceutical residues, have been shown in previous studies.[22] Different kinds of agricultural chemicals, as well as their intermediate metabolites, may co-occur in aquatic environments. Synergistic toxicity of CPF and TCP mixture has been preliminarily observed in aquatic organisms,[23] and it might be implemented

Received: January 7, 2026
Revised: May 15, 2026
Accepted: May 19, 2026
Published: May 25, 2026

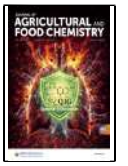

via combined inhibition of antioxidant activity, or due to enhanced bioavailability.[24] However, the mechanisms underlying the interactive effects of their mixture, as well as other pesticide-metabolite mixtures, remain inadequately characterized. To fill the gap, single and combined effects of CPF and its intermediate metabolite TCP, on the blood physiology of *C. auratus* were investigated in this study. First, in silico toxicology platform was employed to predict the absorption, distribution, metabolism, excretion, and toxicity (ADMET) of CPF and TCP, thereby providing mechanistic hypotheses prior to in vivo validation. Then, *C. auratus* individuals were exposed to environmentally relevant concentrations of CPF, TCP, or their mixture, and a series of physiological indices (hematological parameters, erythrocyte membrane integrity, immune activation, and metabolomic response) were systematically measured. Accordingly, differential toxic effects of CPF and TCP, and synergistic effects (i.e., increased hematological and immunological toxicity) of CPF + TCP coexposure were expected to be observed in *C. auratus*. Specifically, compared with single exposure, routine hematological parameters, as well as some key pathways related to immune and inflammation responses, such as the nuclear factor kappa-B (NF-κB) signaling pathway, would be more intensely affected by CPF + TCP coexposure. This study aimed to explore potential mechanisms underlying such synergistic effects based on the alterations in blood physiological parameters. Our findings would yield novel insights into potential synergistic mechanisms and environmental implications of CPF + TCP coexposure, and advance our understanding of the combined effects of pesticides and their metabolites on nontargeted aquatic organisms.

2. MATERIAL AND METHODS

2.1. Preliminary Analysis of CPF and TCP Toxicity

The structural information on CPF and TCP was obtained from the PubChem database and imported into ProTox-II (https://tox.charite.de/protox3/) to make a preliminary prediction of the toxicity of CPF and TCP based on the integration of the network-search algorithm. Using the SwissTarget prediction platform (http://swisstargetprediction.ch/), associated target data were obtained by entering the simplified molecular input line entry system (SMILES) structures of CPF and TCP. Their SMILES structures were submitted to the admetSAR platform (https://lmmd.ecust.edu.cn/admetsar3/index.php) for predicting the ADMET properties.

2.2. Experimental Reagents and Animals

CPF (CAS no. 2921−88−2) and TCP (CAS no. 6515−38−4) used in the experiment were obtained from the Sinopharm Chemical Reagent Co. Ltd. (Shanghai, China), and dissolved in dimethyl sulfoxide (DMSO). A total of 16 fish [mean ± standard error (SE) = 351.5 ± 20.3 g] were obtained from a local aquaculture supplier in Hangzhou (Zhejiang, China), and equally divided into four treatment groups (4 individuals per group): 0 μg/L CPF/TCP (hereinafter referred to as the CK group), nominal 50 μg/L CPF (CPF group), 50 μg/L TCP (TCP group), and 25 μg/L CPF + 25 μg/L TCP (CPF + TCP group). Based on practical constraints, a relatively small sample size was used in this study. The concentration of 25 μg/L was selected based on detected concentrations of CPF and TCP in natural aquatic environments,[7] while 50 μg/L of CPF or TCP was used to facilitate comparing differences between single and combined exposure. Fish were reared in 30 L tanks with gentle ventilation. Tanks were kept in a room at 25 °C, and under a simulated light cycle of 12 h light: 12 h dark. Fish were fed with bloodworms at a ration equivalent to 2% of body weight at 10:00 daily, and acclimated under laboratory conditions for 1 week before exposure. The general parameters in the exposure water were analyzed using a portable water quality analyzer (Shanghai INESA Scientific Instrument Co., Ltd.). No significant differences in quality parameters were observed among groups (water temperature, 26.04 ± 0.23 °C; pH, 7.61 ± 0.04; conductivity, 121.98 ± 0.34 μs/cm; dissolved oxygen, 8.30 ± 0.13 mg/L, ANOVA, all $P > 0.05$). Water samples were collected from each tank, and analyzed for the actual concentrations of CPF and TCP with enzyme-linked immunosorbent assay (ELISA) kits (CPF: #TW-E7316, Shanghai Tongwei Industrial Co., Ltd.; TCP: #DM-K357, Shanghai Duma Biotechnology Co., Ltd.). The measured values were below the detection limit (<0.01 μg/L) in the CK group. The measured CPF and TCP concentrations were 51.21 ± 0.95 μg/L and 49.94 ± 1.34 μg/L, respectively, in the CPF and TCP groups, while 25.20 ± 0.56 μg/L (CPF) and 25.26 ± 1.40 μg/L (TCP) in the CPF + TCP group.

In this study, a 48-h exposure duration was selected to evaluate acute toxic responses in fish under identical experimental conditions. After exposure, blood (approximately 5 mL) was sampled from the caudal vasculature of the fish. Some blood from each individual was transferred into a heparin-coated tube, and used for the measurement of routine parameters, erythrocyte membrane damage, respiratory burst, and gene differential expression. Some blood was allowed to clot at 25 °C, and centrifuged at approximately 1200 × g for 5 min. The supernatants were aliquoted, liquid-nitrogen frozen, and stored at −80 °C, which were subsequently used for metabolomic analysis. Animal procedures in this study complied with the current laws on animal welfare and research in China, and were approved by the Animal Care and Ethics Committee of Hangzhou Normal University (Ethics Approval Number: 2024052).

2.3. Routine Blood Parameters

The blood sample was gently rocked to prevent coagulation and then loaded onto a hemocytometer. The number of white blood cells (WBC) was counted, and different WBC types, namely neutrophils (Neu), lymphocytes (Lym), and monocytes (Mon), were identified, with their percentages in the total WBC count were calculated. A routine blood test was performed using a five-part differential hematology analyzer (DF55 Vet, Shenzhen Dymind Biotechnology Co., Ltd., China). Approximately 20 μL of blood was automatically processed by the instrument using proprietary reagents: hemolytic reagents LYF-1 (100 mL) and LYF-2 (200 mL), diluent DIL-F (10 L), and cleaning solution CLE-P (50 mL). Routine blood parameters, such as red blood cell (RBC) and platelet count (PLT), standard deviation (RDW-SD) and coefficient of variation (RDW-CV) for RBC distribution width, hemoglobin (HGB), mean corpuscular hemoglobin (MCH) and its concentration (MCHC), mean corpuscular volume (MCV), and platelet volume (MPV), platelet distribution width (PDW), hematocrit (HCT), and plateletcrit (PCT), were included. HGB concentration was determined using a noncyanide colorimetric method.

2.4. Erythrocyte Membrane Damage

Erythrocyte membrane damage was evaluated by the frequency of abnormal cell membranes in RBCs. Twenty μL of blood from each sample was collected, and stained with Wright-Giemsa for 30 min after being air-dried naturally and fixed with anhydrous ethanol. A light microscope was used to examine blood smears, and the presence of membrane defects was scored in 1000 erythrocytes.

2.5. Respiratory Burst Activity

Respiratory burst reflects the rapid release of reactive oxygen species (ROS) due to remarkably increased oxygen consumption by immune cells in response to stimulation. Approximately 100 μL of blood was mixed with an equal volume of 0.2% nitroblue tetrazolium (NBT, Sigma Chemical Co., St. Louis, MO, USA) prepared in phosphate-buffered saline. The mixture was thoroughly homogenized and incubated at 25 °C for 30 min. Following incubation, the sample was homogenized again, 50 μL of the resultant solution was transferred into a new tube containing 1 mL of *N*,*N*-dimethylformamide, then vortexed and centrifuged at approximately 1200 × g for 5 min. The supernatant was extracted, and its optical density was measured at 540 nm using a spectrophotometer. The procedure was identical for the

https://doi.org/10.1021/acs.jafc.6c00369
J. Agric. Food Chem. 2026, 74, 16553−16562

Table 1. Primers for qRT-PCR in the Present Study

		Primers	
Gene	Genbank ID	Forward	Reverse
TLR2	XM_026258986	TTCAACCAAAGATTTCCCCAA	GAACAAAGCACTAAGACAGCAGG
TLR4	XM_026278865	AGTTCTTTTATCACTCTTGGTTTAC	CACTTTCTTAGTCTTCGTCTCTTC
p105	XM_026225071	ATCCAGGTGCGGTTTTATG	GCTTGGGTTCACTCGTTTC
TNFα	XM_026290186	CAGGCTTTTGTTTCAGGTGG	GGCAGGAGTTCTGTGGTGGT
IFNG1	XM_026210476	CAGGCTTTTGTTTCAGGTGG	ACAGGTCTTCAGTGTCAGTCGC
IL-1β2	XM_026220359	ACAGAGCAACAAACAAAGCGA	ATCAGAGCGGGGGAAGAAC
IL-6	XM_026289279	TGGATGCAGTGCCTGTCTA	CACGAATCTGTGCTGAAGTTT
EF-1α	XM_026231735	CTCCACCGAGCCCCCTTA	CCCCATGCCATCCAGAAA

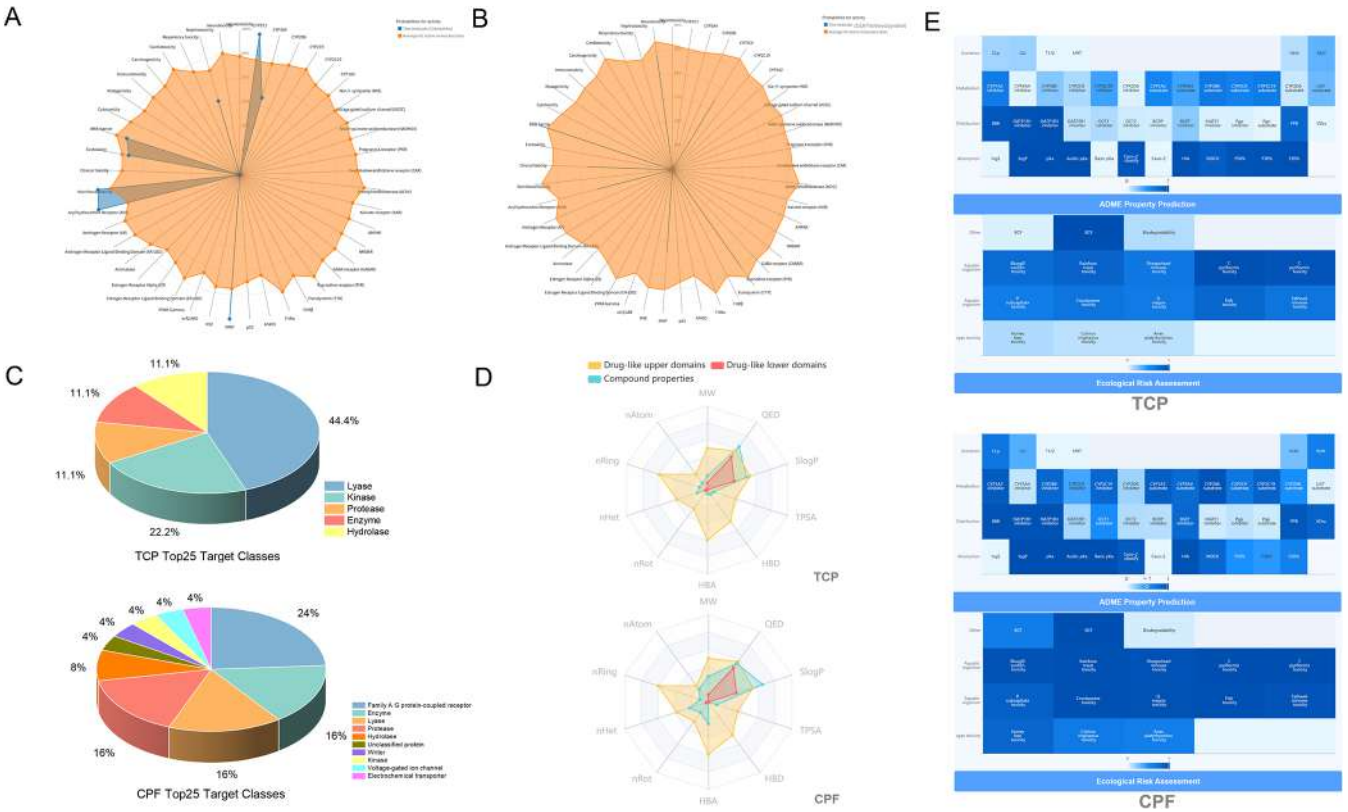

Figure 1. Predictions of network toxicology (A, B). The toxicity radar charts of CPF and TCP, based on network toxicology predictions (C). The top 25 predicted target classes of CPF and TCP, according to SwissTarget prediction analysis (D). Basic physicochemical properties of CPF and TCP, including lipophilicity and solubility (E). ADME property prediction and ecological risk assessment of CPF and TCP, based on in silico models.

CK group, except that the NBT solution was replaced with distilled water.

2.6. Gene Expression Analysis

Some immune- and inflammation-related genes linked to the NF-κB signaling pathway were selected for differential expression analysis. Toll-like receptors (TLR2 and TLR4) are key pattern recognition receptors that detect external stimuli and initiate downstream signaling through the NF-κB pathway. The nuclear factor, NF-kappa-B p105 (p105), serves as a major inhibitory regulator within the NF-κB signaling cascade. Proinflammatory cytokines, such as tumor necrosis factor-α (TNFα), interferon gamma 1 (IFNG1), interleukin-1β (IL-1β2), and interleukin-6 (IL-6), are key modulators of inflammation, and their transcription levels can be upregulated by the activation of the NF-κB pathway. To analyze the differential expression of related genes, such as *TLR2*, *TLR4*, *p105* (*LOC113057632*), *TNFα*, *IFNG1*, *IL-1β2*, and *IL-6* (*LOC113119662*) would be conducive to understanding immune activation and inflammatory responses following exposure. The GenBank IDs of these genes and their primer sequences for amplification are presented in Table 1.

One portion of fresh blood was mixed with 3 volumes of Buffer RZ to ensure complete cell lysis. The mixture was vigorously vortexed and incubated at the room temperature for 5 min to allow complete dissociation of nucleoprotein complexes. To eliminate cellular debris and potential contaminants, the lysate was centrifuged at approximately 13 000 × g at 4 °C for 5 min, and the resultant supernatant was transferred into an RNase-free centrifuge tube. Total RNA from blood samples was extracted using the RNAsimple Total RNA Kit (Tiangen Biotech Co., Ltd., Beijing, China). 200 μL of chloroform was added into, followed by shaking for 15 s and incubating at room temperature for 3 min. After being centrifuged at approximately 13 000 × g at 4 °C for 10 min, the upper aqueous phase containing RNA was carefully collected and transferred into a new RNase-free tube for subsequent purification. For cDNA synthesis, 1 μL of random primer (100 μM) was added to the RNA sample, which was incubated at 70 °C for 10 min and chilled on ice for 2 min. Then, 13 μL of denatured total RNA, 4 μL of 5× RT buffer, 1 μL of dNTPs (10 mM

https://doi.org/10.1021/acs.jafc.6c00369
J. Agric. Food Chem. 2026, 74, 16553−16562

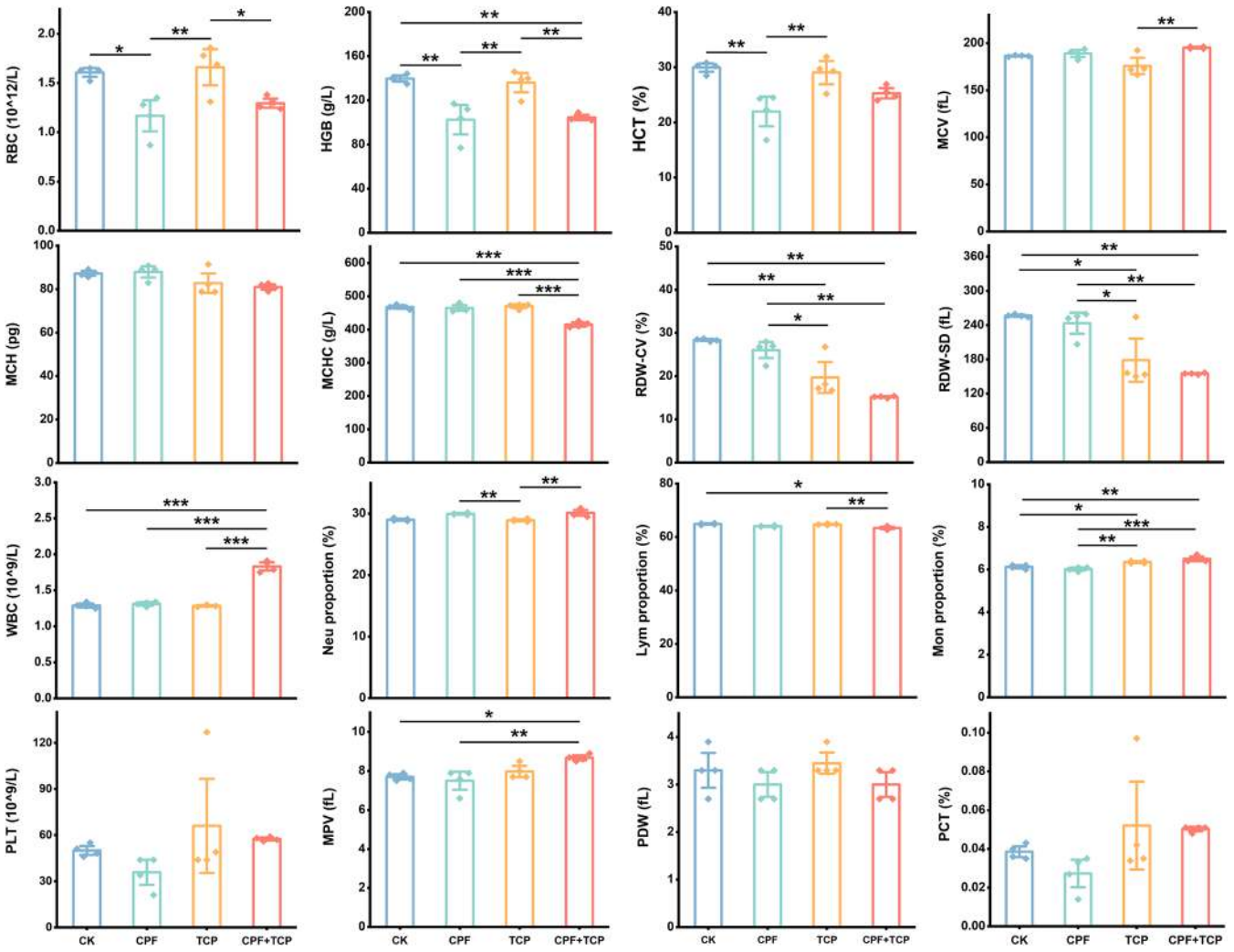

Figure 2. Hematological parameters of *Carassius auratus* after 48-h exposure to CPF, TCP, or CPF + TCP mixture. Sixteen indices were presented as mean values ± SE, including RBC, HGB, HCT, MCV, MCH, MCHC, RDW-CV, RDW-SD, WBC, Neu, Lym, Mon, PLT, MPV, PDW, and PCT. Asterisks indicated significant differences between groups (*$P < 0.05$, **$P < 0.01$, ***$P < 0.001$).

each), 1 μL of RNase inhibitor (40 U/μL), and 1 μL of M-MLV reverse transcriptase (200 U/μL) were mixed. The reaction mixture was incubated at 42 °C for 60 min, followed by enzyme inactivation at 70 °C for 15 min, and then maintained at 4 °C. Quantitative real-time PCR (qRT-PCR) was performed on a 7900HT Real-Time PCR System (Thermo Fisher Scientific Inc., USA) using a 10 μL reaction volume containing 1 μL of synthesized cDNA, 5 μL of 2× SYBR Green Pro TaqHS Premix, 0.2 μL of 50× ROX Reference Dye, 3 μL of ddH2O, and 0.8 μL of primer mix (10 μM). The amplification protocol was as follows: initial denaturation at 95 °C for 1 min, followed by 40 cycles of 95 °C for 10 s and 60 °C for 60 s. Relative gene expression levels were determined using the $2^{-\Delta\Delta CT}$ method.

2.7. Serum Metabolomic Analysis

After being thawed, serum samples (50 μL) were mixed with methanol (400 μL), then vortexed for 1 min, and centrifuged at approximately 13 000 × g at 4 °C for 10 min. Supernatants were concentrated and dried, and their residues were reconstituted in an 80% methanol/water solution (150 μL) with an internal standard of 2-chloro-L-phenylalanine, and then filtered through a 0.22 μm membrane. Liquid chromatography−mass spectrometry (LC-MS) analysis was performed on a Vanquish UHPLC system coupled to a mass spectrometer (Orbitrap Exploris 120, Thermo Fisher Scientific Inc., USA), and completed by the Hangzhou Kaitai Biotechnology Co., Ltd. (Hangzhou, China).

2.8. Data Processing and Analysis

One-way analysis of variance (ANOVA, the Cohen's *f* value was presented as the measure of effect size) was performed to examine among-group differences in erythrocyte membrane abnormality rates, respiratory burst activity, hematological parameters, gene expression levels, and spectral areas of identified serum metabolites, with Tukey's test for pairwise comparisons. For metabolomic profiling, principal component analysis (PCA) was performed to examine among-group variation. Metabolite identification was performed by referencing publicly available databases such as MASSBANK, METLIN, and HMDB. A statistical significance criterion of $P < 0.05$ and a variable importance in projection (*VIP*) score >1 (from orthogonal partial least-squares discriminant analysis) were used to determine differential metabolites. Hierarchical clustering heatmaps were used to visualize group-specific patterns of differential metabolites, and KEGG enrichment analysis was performed to identify differential metabolic pathways. Prior to statistical testing, data distribution and homogeneity of variance were detected using the Kolmogorov−Smirnov test and Bartlett's test, respectively. Some variables (e.g., relative expression levels of *TNFα*, *IFNG1*, *IL-1β2*, and *IL-6*) were square-root transformed before ANOVA. Nonparametric tests (Kruskal−Wallis and Mann−Whitney tests) were performed if parametric assumptions were not satisfied.

https://doi.org/10.1021/acs.jafc.6c00369
J. Agric. Food Chem. 2026, 74, 16553−16562

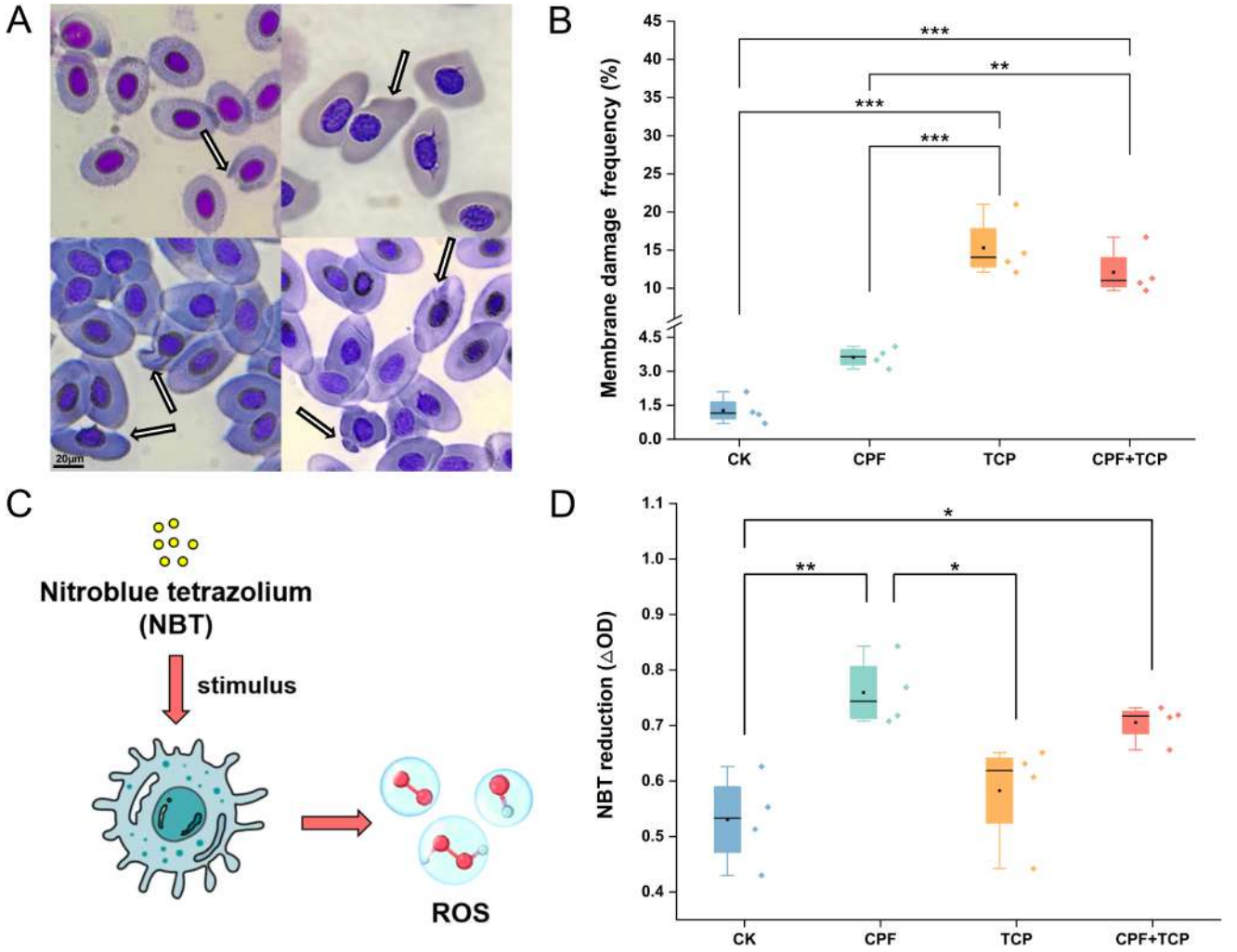

Figure 3. Erythrocyte membrane damage and respiratory burst activity. Photos of a red blood cell under a microscope, with an arrow pointing to an example of a cell with an abnormal membrane (A). Boxplots for the frequency of abnormal red blood cell membrane morphology (B). NBT stimulates cells to produce ROS (C). Boxplots for respiratory burst activity (D). Asterisks indicated significant differences between groups (*P < 0.05, **P < 0.01, ***P < 0.001).

3. RESULTS

3.1. In Silico Toxicity Prediction of CPF and TCP

The ProTox-II platform showed that CPF would have high probabilities (77−97%) of predicted activity in ecotoxicity and nutritional toxicity, whereas TCP had potential neurotoxicity and clinical toxicity (Figure 1A, B). CPF and TCP might be inactive in carcinogenicity, immunotoxicity, mutagenicity, and most nuclear receptor signaling and stress response pathways, except for mitochondrial membrane potential (MMP, CPF: 1.00; TCP: 0.54). CPF also showed the activation property of the aryl hydrocarbon receptor (AhR), whereas the engagement of TCP in AhR activation was weak.

Target class distribution by SwissTarget prediction revealed that CPF mainly interacted with family A G protein-coupled receptors (24%), enzymes (16%), lyases (16%), proteases (16%), and hydrolases (8%). In contrast, TCP targets were classified as lyases (44.4%), kinases (22.2%), proteases (11.1%), and enzymes (11.1%), indicating distinct molecular interaction profiles between these two compounds (Figure 1C).

The basic properties of CPF and TCP were shown in Figure 1D. Predicted ADMET properties by the admetSAR platform showed that both CPF and TCP had high intestinal absorption probabilities (HIA > 97%) and were permeable to the blood−brain barrier (CPF: 97.8%; TCP: 93.4%). CPF showed a higher lipophilicity (log$P$ = 5.37) compared with TCP (log$P$ = 2.53), but lower water solubility (log$S$ = −5.93 vs −3.00). CPF was identified as an inhibitor and substrate of multiple cytochrome P450 isoenzymes (CYP1A2, CYP2B6, CYP2C19), while TCP showed fewer interactions, suggesting that CPF might present more complex metabolic profiles. Notably, both compounds were predicted to be nonbiodegradable and exhibited high ecological toxicity toward aquatic organisms, such as protozoa, crustaceans, and fish, with prediction probabilities >80% (Figure 1E).

3.2. Blood Routine Parameters

The hematological parameters of *C. auratus* after a 48-h exposure were presented in Figure 2. Compared with the CK group, CPF + TCP exposed group exhibited significant alterations in multiple blood indices, including HGB ($F_{3, 12}$ = 13.24, P < 0.001, Cohen's f = 1.82), MCHC ($F_{3, 12}$ = 37.74, P < 0.001, Cohen's f = 3.07), RDW-CV ($F_{3, 12}$ = 19.84, P < 0.001, Cohen's f = 2.23), and RDW-SD ($F_{3, 12}$ = 12.25, P < 0.01, Cohen's f = 1.75). These indices were significantly

https://doi.org/10.1021/acs.jafc.6c00369
J. Agric. Food Chem. 2026, 74, 16553−16562

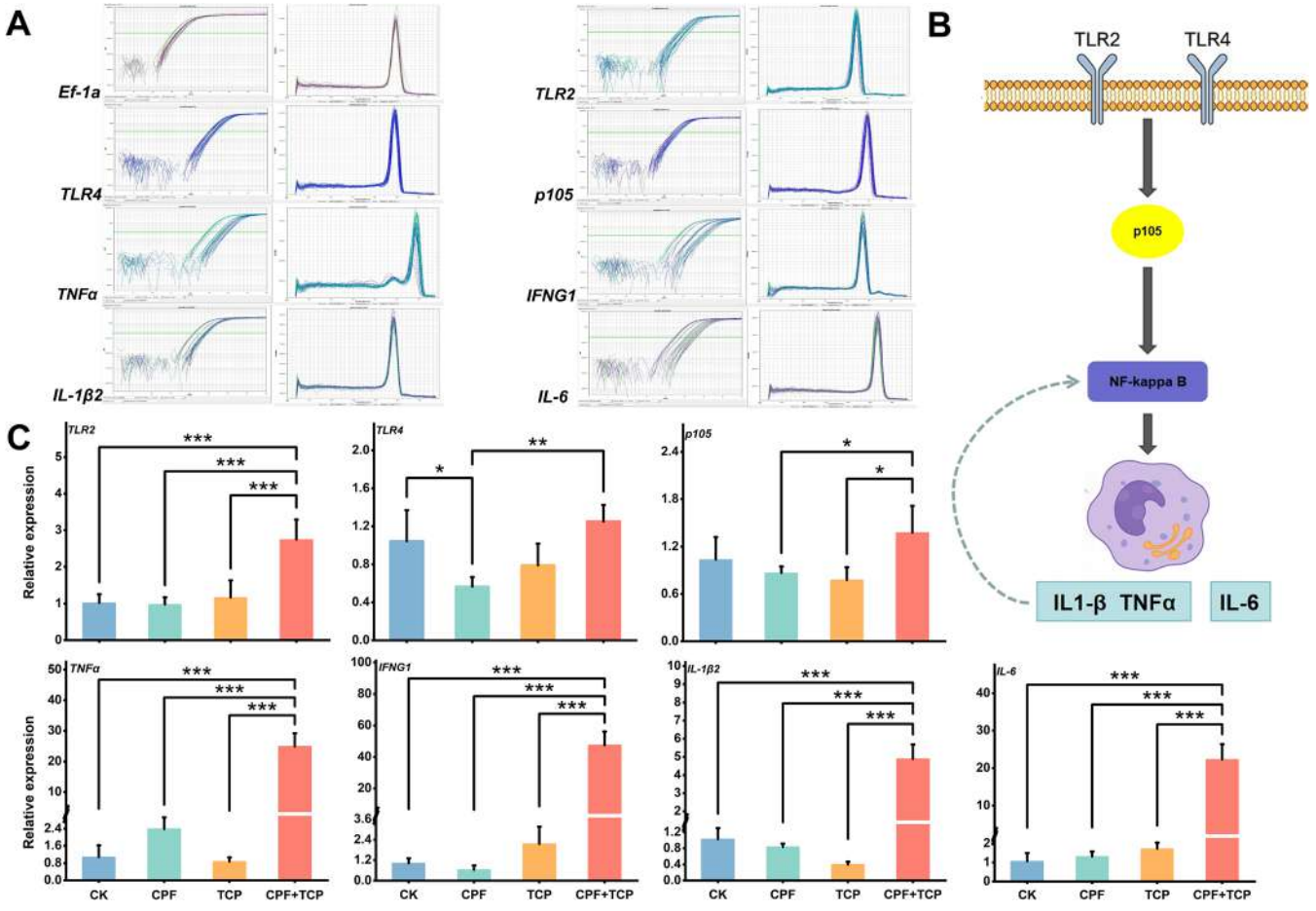

Figure 4. Amplification curve and melting curve for each gene (A). Toll-like receptor (TLR) signaling pathway and downstream NF-κB activation (B). Mean values (+SE) for relative expression levels of genes (*TLR2*, *TLR4*, *p105*, *TNFα*, *IFNG1*, *IL-1β2*, and *IL-6*) (C). Asterisks indicated significant differences between groups (*$P < 0.05$, **$P < 0.01$, ***$P < 0.001$).

decreased following combined exposure. Additionally, combined exposure led to a marked increase in total WBC counts ($F_{3, 12} = 141.64$, $P < 0.001$, Cohen's $f = 5.95$), accompanied by a significant increase in Mon proportion ($F_{3, 12} = 17.76$, $P < 0.001$, Cohen's $f = 2.11$), while Lym proportion ($F_{3, 12} = 9.49$, $P < 0.01$, Cohen's $f = 1.54$) significantly decreased. Platelet-related parameters, such as MPV ($F_{3, 12} = 7.21$, $P < 0.01$, Cohen's $f = 1.34$), also showed a significant increase in the CPF + TCP group compared to the CK group.

For single exposure, TCP treatment alone resulted in significant alterations in RDW-CV, RDW-SD, and Mon proportion, whereas CPF exposure showed effects on RBC count ($F_{3, 12} = 8.21$, $P < 0.01$, Cohen's $f = 1.43$), HGB, and HCT ($F_{3, 12} = 9.23$, $P < 0.01$, Cohen's $f = 1.52$)(Figure 2). However, the magnitude of changes observed in the CPF + TCP combined group was greater than those in the single-exposure groups.

3.3. Erythrocyte Membrane Damage and Respiratory Burst Activity

TCP and CPF + TCP exposure caused a remarkable increase in the frequency of erythrocyte membrane damage, being 12 and 9.49 times higher than that of the CK group, respectively (square-root transformed data, $F_{3, 12} = 54.93$, $P < 0.001$, Cohen's $f = 3.71$, Figure 3A, B). As shown in Figure 3D, the respiratory burst activity of WBCs was significantly higher in the CPF and CPF + TCP-exposed groups than in the CK group ($F_{3, 12} = 8.67$, $P < 0.01$, Cohen's $f = 1.47$).

3.4. Relative Expression of Immune- and Inflammation-Related Genes

The mRNA expression levels of key immune- and inflammation-related genes (*TLR2*, *TLR4*, *p105*, *TNFα*, *IFNG1*, *IL-1β2*, and *IL-6*) in whole blood after 48 h of exposure re were shown in Figure 4. Compared with the CK group, the transcription levels of *TLR2* ($F_{3, 12} = 15.03$, $P < 0.001$, Cohen's $f = 1.94$), as well as proinflammatory cytokines, *TNFα* (square-root transformed data, $F_{3, 12} = 201.97$, $P < 0.001$, Cohen's $f = 7.11$), *IFNG1* ($F_{3, 12} = 241.82$, $P < 0.001$, Cohen's $f = 7.78$), *IL-1β2* ($F_{3, 12} = 135.06$, $P < 0.001$, Cohen's $f = 5.81$), and *IL-6* ($F_{3, 12} = 200.55$, $P < 0.001$, Cohen's $f = 7.08$), were markedly upregulated in the CPF + TCP group, but not in the CPF or TCP group. The expression of *TLR4* ($F_{3, 12} = 7.95$, $P < 0.01$, Cohen's $f = 1.41$) and *p105* ($F_{3, 12} = 4.34$, $P = 0.027$, Cohen's $f = 1.04$) in the CPF + TCP group was significantly higher than those in the single-exposure groups.

3.5. Serum Metabolomic Profile

The first two components of PCA accounted for more than 60% of the total variance (62.53% and 66.28% for the positive and negative ion modes, respectively). Clear among-group differences in the serum metabolomic profile were demonstrated by PCA (Figure 5A,B), as well as by heatmap cluster analysis (Figure 5C,D). According to the available database, a

https://doi.org/10.1021/acs.jafc.6c00369
J. Agric. Food Chem. 2026, 74, 16553−16562

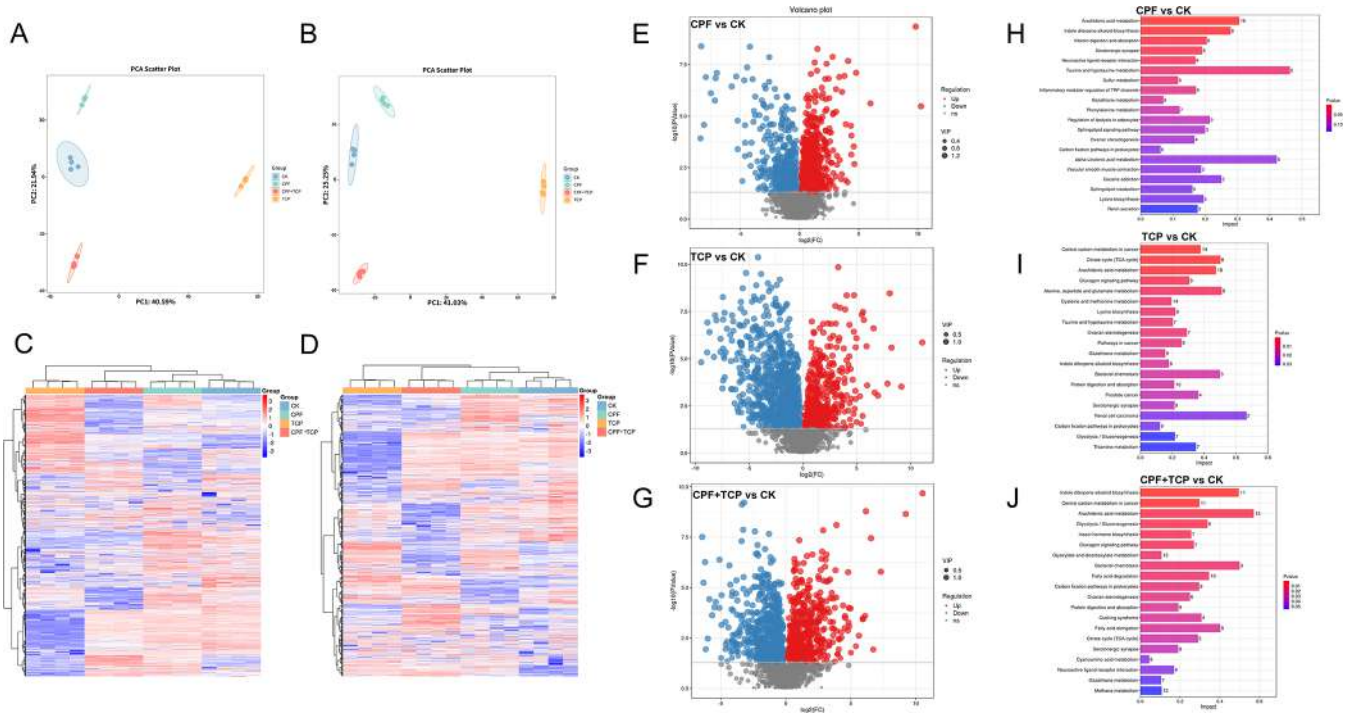

Figure 5. Differential serum metabolites in *Carassius auratus*. Score plots for principal component analysis on serum metabolomic profiles in the positive (A) and negative ion mode (B). Heatmap cluster analysis in the positive (C) and negative ion mode (D). Volcano plots between the control and CPF-exposed group (E), between the control and TCP-exposed group (F), and between the control and CPF + TCP-exposed group (G). Cylindrical diagram of metabolic pathway influencing factors between the CPF-exposed (H), TCP-exposed (I), CPF + TCP-exposed group (J), and the control group.

total of 2543 metabolites were identified. Compared with the CK group, there were 906, 1190, and 1097 differential metabolites in the CPF, TCP, and CPF + TCP groups, respectively. Some inflammation-related metabolites were significantly changed in the CPF + TCP group [e.g., prostaglandin E2, leukotriene A4 (LTA4), 15 (S)-HPETE, lipoxin A4, and LTB4_20-hydroxy] (Figure 5E,F,G). Multiple enriched KEGG pathways were shown to change significantly in the exposed groups. Some specific pathways and metabolites changed significantly. For instance, metabolic pathways related to energy metabolism [e.g., central carbon metabolism in cancer, tricarboxylic acid (TCA) cycle, glycolysis/gluconeogenesis] and lipid metabolism (degradation and elongation of fatty acids, arachidonic acid metabolism), as well as other pathways associated with inflammation, signaling, etc. [e.g., sulfur metabolism, inflammatory mediator regulation of TRP channels, glucagon signaling pathway, ovarian steroidogenesis, thiamine metabolism, D-amino acid metabolism], were significantly altered in exposed fish (Figure 5H,I,J).

4. DISCUSSION

4.1. Discrepant Effects of CPF and TCP Exposure

In this study, clear alterations in blood physiological and biochemical indices after exposure to a pesticide-CPF and its primary metabolite-TCP could be observed in a common freshwater fish species, *C. auratus*, which reflects potential hematologic toxicity induced by CPF, TCP, as well as the mixture of them. A small sample size (4 replicates per group in this study) may lead to high variability. However, our measured variables with significant differences (e.g., frequency of abnormal cell membranes, respiratory burst activity, and some blood routine parameters) showed large effect sizes (Cohen's $f > 0.94$) and achieved statistical powers (>0.77), which should be sufficient to detect among-group differences in these variables with the sample size of 4. It is noteworthy that these alterations differed between CPF and TCP exposure, as well as from their mixture exposure, probably implying discrepant toxic effects between CPF and its intermediate metabolite, and novel combined toxicity under exposure to CPF co-occurring with its metabolite.

The ProTox-II and admetSAR platforms predicted that CPF would exhibit high probabilities of ecotoxicity along with strong MMP disruption. The in vivo responses to CPF exposure in *C. auratus* were consistent with the predicted effects. Enhanced respiratory burst activity of WBCs potentially indicated an acceleration of oxidative metabolism and an activated immune response, which might lead to excessive ROS formation and induce oxidative stress.[25] MMP disruption is a central feature of mitochondrial dysfunction. It was strongly predicted and might further promote the production of excessive ROS.[26] Altered hematological parameters, e.g., decreased RBC, HGB, and HCT levels, probably resulted from CPF-induced inhibition of hematopoiesis or anoxia. Pathway enrichment analysis revealed that CPF led to significant perturbations of sulfur metabolism and the inflammatory mediator regulation of TRP channels. Sulfur plays an important role in the oxidation−reduction process of organisms.[27] The perturbation of sulfur metabolism might damage the antioxidant defense system and thus exacerbate oxidative stress.[28] TRP channels are involved in sensory transduction and immune regulation. The involvement of CPF in triggering proinflammatory signaling might also be supported by the modulation of TRP channels.[29] In line with the computationally predicted toxicological profile, CPF

https://doi.org/10.1021/acs.jafc.6c00369
J. Agric. Food Chem. 2026, 74, 16553−16562

exposure would elicit systemic toxic effects, characterized by hematological impairment, oxidative stress, and metabolic perturbation in *C. auratus*.

TCP exposure also resulted in obvious hematological perturbations in *C. auratus*. TCP induced substantial erythrocyte membrane damage, with RBC abnormality increasing by more than 12-fold compared to the CK. The membrane integrity is crucial for cellular function and closely related to the removal efficiency of toxic matter from cells. Additionally, plasma membrane damage might result in the impairment of oxygen transport and acceleration of RBC aging, and these effects might be associated with oxidative or inflammatory stress.[30,31] Compared with the CK group, altered hematological parameters, e.g., decreased RDW-CV and RDW-SD, but increased Mon, potentially suggested TCP-induced erythropoietic imbalance and immunomodulatory effects,[32,33] although there was no obvious alteration in the RBC count. Multiple metabolic pathways that are involved in energy regulation, vitamin utilization, and innate immune defense (e.g., glucagon signaling pathway, thiamine and D-amino acid metabolism, etc.) were shown to be disrupted by TCP exposure.[34−36] In line with predicted effects, as an intermediate metabolite of CPF, TCP still retains somewhat bioactivity, and its exposure would cause considerable structural, functional, and metabolic alterations in the blood of *C. auratus*. Certainly, the toxic effects of TCP might be different from those of CPF, which could be indicated by nonoverlapping molecular targets from in silico prediction, but also by our differential findings. CPF exposure significantly elevated respiratory burst activity and altered inflammatory-related pathways, whereas TCP might damage the erythrocyte membrane and lead to erythropoietic imbalance.

4.2. Combined Effects of CPF + TCP Mixture

A somewhat unique pattern of perturbative effect on blood physiology appeared to be exhibited in the CPF + TCP combined group, differing from that of CPF or TCP exposure alone. This could be reflected by obvious separations between the CPF + TCP group and other groups from multivariate statistical analysis, as well as by significant alterations in some hematological parameters. Compared with the CK group, the membrane abnormality of RBCs and the respiratory burst activity of WBCs significantly increased in the CPF + TCP group, probably indicating induced oxidative or inflammatory stress. The combined effects of the CPF + TCP mixture on blood physiology might be more extensive. For instance, alterations in some blood routine parameters, e.g., decreased HGB, MCHC, RDW-CV, and RDW-SD, increased WBC count and Mon proportion, and decreased Lym proportion, potentially suggested erythropoietic impairment, immune activation, and inflammation.[32,37] The alterations of neutrophils and lymphocytes are usually associated with an inflammatory response, and immune dysregulation may lead to excessive inflammation.[37,38] Moreover, increased MPV probably indicated platelet activation or systemic inflammatory stress.[39]

Furthermore, some enriched metabolic pathways related to energy and lipid metabolism, and inflammation, e.g., glycolysis/gluconeogenesis, TCA cycle, fatty acid degradation and elongation, and arachidonic acid metabolism, were perturbed significantly by CPF + TCP combined exposure, but not necessarily by CPF or TCP exposure alone. These metabolic responses are likely to be linked to oxidative or inflammatory stress.[40,41]

4.3. Synergistic Activation of Immune Pathways

Interestingly, our results revealed that more pronounced innate immune pathway activation might be triggered by CPF + TCP combined exposure in *C. auratus*. Immune- and inflammation-related genes, e.g., *TLR2*, *TLR4*, *p105*, *TNFα*, *IFNG1*, *IL-1β2*, and *IL-6*, were shown to be significantly upregulated. These genes serve as critical mediators of innate immune responses and inflammatory cytokine production.[42−45] The upregulation of *TLR2* and *TLR4* suggested that combined exposure enhanced pathogen recognition-like responses, probably through damage-associated molecular patterns (DAMPs), as reflected from hematological alterations, such as RBC membrane damage.[46] The activation of *p105*, *TNF-α*, *IFNG1*, *IL-1β2*, and *IL-6* might further imply a robust immune response and the onset of systemic inflammation.[44,45,47] Contrarily, the expressions of these genes were not altered after CPF or TCP exposure alone. Although immune activation and inflammation caused by single exposure were reflected in alterations in some hematological parameters, their effects were clearly milder than those of CPF + TCP combined exposure. Accordingly, we speculated that the intermediate metabolite of CPF, TCP, could potentially modulate or amplify CPF-induced oxidative stress and inflammation in a mixture context.

Activation of innate immune pathways may also manifest through alterations in serum metabolites, which are associated with inflammation, such as prostaglandin E2, LTA4, 15(S)-HPETE, lipoxin A4, and LTB4_20-hydroxy. Prostaglandin E2 can modulate immune cell activity, and amplify inflammatory responses by enhancing the expression and secretion of cytokines.[48,49] Similarly, LTA4 is a potent chemoattractant for neutrophils, and can stimulate the production of TNF-α and IL-1.[50] These lipid mediators form a feedback loop with cytokines, and their alterations might contribute to sustained inflammation and immune dysregulation.

Collectively, RBC membrane damage, enhanced respiratory burst, and hematological perturbations induced by CPF + TCP coexposure might function as DAMPs, which could be discerned by TLR2/4 receptors, thereby activating innate immunity. This recognition mediated significant upregulation of proinflammatory cytokine genes (*TNFα*, *IL-1β*, *IL-6*), propagating systemic inflammation. Concomitant disruptions in inflammatory metabolites (e.g., prostaglandins, leukotrienes) further demonstrated downstream immunometabolic dysregulation.

The present study demonstrated that combined exposure to CPF and its intermediate metabolite, TCP, induced synergistic toxic effects, primarily through enhanced activation of innate immune pathways in a common freshwater fish species, *C. auratus*. Compared with single exposure, CPF + TCP coexposure might result in novel and more severe toxic outcomes. These findings highlighted the importance of considering pesticide−metabolite mixtures in environmental risk assessment. However, only 48-h exposure was conducted here, and prevented us from evaluating the long-term health outcomes of animals under exposure to environmentally relevant concentrations of CPF and TCP. To better understand the environmental risks of pesticides and their metabolites, long-term toxic effects, or recovery dynamics

https://doi.org/10.1021/acs.jafc.6c00369
J. Agric. Food Chem. 2026, 74, 16553−16562

and species-specific sensitivities, should be explored in future studies.

■ ASSOCIATED CONTENT

Supporting Information

The Supporting Information is available free of charge at https://pubs.acs.org/doi/10.1021/acs.jafc.6c00369.

(Table S1) List of metabolite identification and quantification; (Table S2) Raw data from qRT-PCR analysis (PDF)

■ AUTHOR INFORMATION

Corresponding Authors

Jian-Rao Hu − *Zhejiang Provincial Key Laboratory of Wetland Intelligent Monitoring and Ecological Restoration, School of Life and Environmental Sciences, Hangzhou Normal University, Hangzhou, Zhejiang 311121, China*; Email: jrhu@hznu.edu.cn

Hong-Liang Lu − *Zhejiang Provincial Key Laboratory of Wetland Intelligent Monitoring and Ecological Restoration, School of Life and Environmental Sciences, Hangzhou Normal University, Hangzhou, Zhejiang 311121, China*; orcid.org/0000-0003-4494-0486; Email: honglianglu@hznu.edu.cn

Authors

Huo-Bin Tang − *Zhejiang Provincial Key Laboratory of Wetland Intelligent Monitoring and Ecological Restoration, School of Life and Environmental Sciences, Hangzhou Normal University, Hangzhou, Zhejiang 311121, China*

Jun-Hao Chen − *Zhejiang Provincial Key Laboratory of Wetland Intelligent Monitoring and Ecological Restoration, School of Life and Environmental Sciences, Hangzhou Normal University, Hangzhou, Zhejiang 311121, China*

Complete contact information is available at: https://pubs.acs.org/10.1021/acs.jafc.6c00369

Author Contributions

H.-B.T.: Conceptualization, Writing—original draft. J.-H.C.: Investigation, Data curation. J.-R.H.: Software, Writing—review and editing. H.-L.L.: Writing—review and editing, Supervision.

Funding

This study was supported by grants from the National Natural Science Foundation of China (32471577) and the XinMiao Talents Program of Zhejiang Province (2025R441A040).

Notes

The authors declare no competing financial interest.

■ ABBREVIATIONS

AChE: acetylcholinesterase; ADMET: absorption, distribution, metabolism, excretion, and toxicity; AhR: aryl hydrocarbon receptor; CPF: chlorpyrifos; DMSO: dimethyl sulfoxide; ELISA: enzyme-linked immunosorbent assay; IL: interleukin; MMP: mitochondrial membrane potential; NBT: nitroblue tetrazolium; NF-κB: nuclear factor kappa-B; qRT-PCR: quantitative real-time polymerase chain reaction; RBC: red blood cell; ROS: reactive oxygen species; TCA: tricarboxylic acid; TCP: 3,5,6-trichloro-2-pyridinol; TLR: toll-like receptor; TNF: tumor necrosis factor; TRP: transient receptor potential; WBC: white blood cell

■ REFERENCES

(1) Sidhu, G. K.; Singh, S.; Kumar, V.; Dhanjal, D. S.; Datta, S.; Singh, J. T. Monitoring and Biodegradation of Organophosphate Pesticides: A Review. *Crit. Rev. Environ. Sci. Technol.* **2019**, *49* (13), 1135−1187.

(2) Dar, M. A.; Kaushik, G.; Villarreal-Chiu, J. F. Pollution Status and Bioremediation of Chlorpyrifos in Environmental Matrices by the Application of Bacterial Communities: A Review. *J. Environ. Manage.* **2019**, *239*, 124−136.

(3) Žabar, R.; Sarakha, M.; Lebedev, A. T.; Polyakova, O. V.; Trebše, P. Photochemical Fate and Photocatalysis of 3,5,6-trichloro-2-pyridinol, Degradation Product of Chlorpyrifos. *Chemosphere* **2016**, *144*, 615−620.

(4) Huang, X.; Cui, H.; Duan, W. Ecotoxicity of Chlorpyrifos to Aquatic Organisms: A Review. *Ecotoxicol. Environ. Saf.* **2020**, *200*, 110731.

(5) Ubaid Ur Rahman, H.; Asghar, W.; Nazir, W.; Sandhu, M. A.; Ahmed, A.; Khalid, N. A Comprehensive Review on Chlorpyrifos Toxicity with Special Reference to Endocrine Disruption: Evidence of Mechanisms, Exposures and Mitigation Strategies. *Sci. Total Environ.* **2021**, *755*, 142649.

(6) Jeon, H. J.; Cho, Y.; Kim, K.; Kim, C.; Lee, S. E. Combined Toxicity of 3,5,6-trichloro-2-pyridinol and 2-(bromomethyl)-naphthalene in the Early Stages of Zebrafish (*Danio rerio*) Embryos: Abnormal Heart Development at Lower Concentrations via Differential Expression of Heart Forming-related Genes. *Environ. Pollut.* **2023**, *325*, 121450.

(7) Wang, A.; Liu, Y.; Yan, Y.; Jiang, Y.; Shi, S.; Wang, J.; Qiao, K.; Yang, L.; Wang, S.; Li, S.; Gui, W. Chlorpyrifos Influences Tadpole Development by Disrupting Thyroid Hormone Signaling Pathways. *Environ. Sci. Technol.* **2025**, *59* (1), 142−151.

(8) Guo, Y.; Wu, C.; Hu, S. Y.; Xie, Y. X.; Wu, W. Y.; Li, B. X.; Chen, Y. T.; Hui, C. Y. ChpR-displaying Bacteria for Bioremediation of Chlorpyrifos and TCP: A Whole-cell Biosorbent Approach. *Water Res.* **2025**, *283*, 123775.

(9) Shaffo, F. C.; Grodzki, A. C.; Schelegle, E. S.; Lein, P. J. The Organophosphorus Pesticide Chlorpyrifos Induces Sex-specific Airway Hyperreactivity in Adult Rats. *Toxicol. Sci.* **2018**, *165* (1), 244−253.

(10) Gómez-Canela, C.; Prats, E.; Piña, B.; Tauler, R. Assessment of Chlorpyrifos Toxic Effects in Zebrafish (*Danio rerio*) Metabolism. *Environ. Pollut.* **2017**, *220*, 1231−1243.

(11) Lu, S.; Liu, S.; Cui, J.; Liu, X.; Zhao, C.; Fan, L.; Yin, S.; Hu, H. Combination of Patulin and Chlorpyrifos Synergistically Induces Hepatotoxicity via Inhibition of Catalase Activity and Generation of Reactive Oxygen Species. *J. Agric. Food Chem.* **2019**, *67* (41), 11474−11480.

(12) Bai, J.; Deng, S.; Fu, H.; Yang, Q.; Ren, F.; Zeng, S.; Chen, Z.; Yang, Y.; Wu, Z. Chlorpyrifos Induces Placental Oxidative Stress and Barrier Dysfunction by Inducing Mitochondrial Apoptosis through the ERK/MAPK Signaling Pathway: In vitro and in vivo Studies. *Sci. Total Environ.* **2023**, *903*, 166449.

(13) Cáceres, T.; He, W.; Naidu, R.; Megharaj, M. Toxicity of Chlorpyrifos and TCP alone and in Combination to *Daphnia carinata*: The Influence of Microbial Degradation in Natural Water. *Water Res.* **2007**, *41* (19), 4497−4503.

(14) Echeverri-Jaramillo, G.; Jaramillo-Colorado, B.; Sabater-Marco, C.; Castillo-López, M.-A. Cytotoxic and Estrogenic Activity of Chlorpyrifos and its Metabolite 3. *Ecotoxicology* **2021**, *30* (1), 104−117.

(15) Lin, W.; Guo, H.; Wang, L.; Zhang, D.; Wu, X.; Li, L.; Qiu, Y.; Yang, L.; Li, D.; Tang, R. Parental Transfer of Microcystin-LR-induced Innate Immune Dysfunction of Zebrafish: A Cross-generational Study. *Environ. Sci. Technol.* **2020**, *54* (2), 1014−1023.

(16) Chen, H.; Wang, L.; Zhao, X.; Jiang, H.; Wu, M.; Ding, Y.; Jia, X.; Zhang, Y.; Li, T.; Zhang, Y.; et al. A Polymer-based Antigen

Carrier Activates Two Innate Immune Pathways for Adjuvant-free Subunit Vaccines. *ACS Nano* **2024**, *18* (12), 9160−9175.
(17) Liu, J.; Lu, G.; Ding, J.; Zhang, Z.; Wang, Y. Tissue distribution, bioconcentration, metabolism, and effects of erythromycin in crucian carp (*Carassius auratus*). *Sci. Total Environ.* **2014**, *490*, 914−920.
(18) Liu, Y.; Chen, Z.; Li, S.; Ding, L.; Wei, X.; Han, S.; Wang, P.; Sun, Y. Multi-omics Profiling and Biochemical Assays Reveal the Acute Toxicity of Environmental Related Concentrations of Di-(2-ethylhexyl) phthalate (DEHP) on the Gill of Crucian Carp (*Carassius auratus*). *Chemosphere* **2022**, *307*, 135814.
(19) Yan, Z.; Wan, J.; Liu, J.; Yao, B.; Lu, Y.; Guo, Z.; Li, Y. α-lipoic acid Ameliorates Hepatotoxicity Induced by Chronic Ammonia Toxicity in Crucian Carp (*Carassius auratus gibelio*) by Alleviating Oxidative Stress, Inflammation and Inhibiting ERS Pathway. *Ecotoxicol. Environ. Saf.* **2023**, *266*, 115533.
(20) Li, X.; Hu, X.; Lv, A.; Guan, Z. Skin Immune Response to *Aeromonas hydrophila* Infection in Crucian Carp *Carassius auratus* Revealed by Multi-omics Analysis. *Fish Shellfish Immunol.* **2022**, *127*, 866−875.
(21) Kim, J. H.; Yu, Y. B.; Choi, J. H. Toxic Effects on Bioaccumulation, Hematological Parameters, Oxidative Stress, Immune Responses and Neurotoxicity in Fish Exposed to Microplastics: A Review. *J. Hazard. Mater.* **2021**, *413*, 125423.
(22) Lu, L.; Shan, C.; Tong, D.; Yu, Y.; Zhang, W.; Zhang, X.; Shu, Y.; Li, W.; Liu, G.; Shi, W. Olfactory Toxicity of Tetrabromobisphenol A to the Goldfish *Carassius auratus*. *J. Hazard. Mater.* **2024**, *479*, 135661.
(23) Echeverri-Jaramillo, G.; Jaramillo-Colorado, B.; Sabater-Marco, C.; Castillo-López, M. Á. Acute Toxicity of Chlorpyrifos and its Metabolite 3,5,6-trichloro-2-pyridinol Alone and in Combination Using a Battery of Bioassays. *Environ. Sci. Pollut. Res.* **2020**, *27* (26), 32770−32778.
(24) Cedergreen, N. Quantifying Synergy: A Systematic Review of Mixture Toxicity Studies within Environmental Toxicology. *PLoS One* **2014**, *9*, No. e96580.
(25) El-Benna, J.; Hurtado-Nedelec, M.; Marzaioli, V.; Marie, J. C.; Gougerot-Pocidalo, M. A.; Dang, P. M. Priming of the Neutrophil Respiratory Burst: Role in Host Defense and Inflammation. *Immunol Rev.* **2016**, *273* (1), 180−193.
(26) Zorova, L. D.; Popkov, V. A.; Plotnikov, E. Y.; Silachev, D. N.; Pevzner, I. B.; Jankauskas, S. S.; Babenko, V. A.; Zorov, S. D.; Balakireva, A. V.; Juhaszova, M.; et al. Mitochondrial Membrane Potential. *Anal. Biochem.* **2018**, *552*, 50−59.
(27) Grein, F.; Ramos, A. R.; Venceslau, S. S.; Pereira, I. A. Unifying Concepts in Anaerobic Respiration: Insights from Dissimilatory Sulfur Metabolism. *Biochim. Biophys. Acta* **2013**, *1827* (2), 145−160.
(28) Nakajima, T. Roles of Sulfur Metabolism and Rhodanese in Detoxification and Anti-oxidative Stress Functions in the Liver: Responses to Radiation Exposure. *Med. Sci. Monit.* **2015**, *21*, 1721−1725.
(29) Silverman, H. A.; Chen, A.; Kravatz, N. L.; Chavan, S. S.; Chang, E. H. Involvement of Neural Transient Receptor Potential Channels in Peripheral Inflammation. *Front. Immunol.* **2020**, *11*, 590261.
(30) Mohanty, J. G.; Nagababu, E.; Rifkind, J. M. Red Blood Cell Oxidative Stress Impairs Oxygen Delivery and Induces Red Blood Cell Aging. *Front. Physiol.* **2014**, *5*, 84.
(31) Gwozdzinski, K.; Pieniazek, A.; Gwozdzinski, L. Reactive Oxygen Species and their Involvement in Red Blood Cell Damage in Chronic Kidney Disease. *Oxid. Med. Cell. Longevity* **2021**, *2021* (1), 6639199.
(32) Salvagno, G. L.; Sanchis-Gomar, F.; Picanza, A.; Lippi, G. Red Blood Cell Distribution Width: A Simple Parameter with Multiple Clinical Applications. *Crit. Rev. Clin. Lab. Sci.* **2015**, *52* (2), 86−105.
(33) Shi, C.; Pamer, E. G. Monocyte Recruitment during Infection and Inflammation. *Nat. Rev. Immunol.* **2011**, *11* (11), 762−774.
(34) Jiang, G.; Zhang, B. B. Glucagon and Regulation of Glucose Metabolism. *Am. J. Physiol. Endocrinol. Metab.* **2003**, *284*, No. E671−E678.
(35) Fan, Y.; Qin, Y.; Chen, M.; Li, X.; Wang, R.; Huang, Z.; Xu, Q.; Yu, M.; Zhang, Y.; Han, X.; et al. Prenatal Low-dose DEHP Exposure Induces Metabolic Adaptation and Obesity: Role of Hepatic Thiamine Metabolism. *J. Hazard. Mater.* **2020**, *385*, 121534.
(36) Sasabe, J.; Suzuki, M. Emerging Role of D-amino Acid Metabolism in the Innate Defense. *Front Microbiol.* **2018**, *9*, 933.
(37) Liu, Y.; Du, X.; Chen, J.; Jin, Y.; Peng, L.; Wang, H. X.; Luo, M.; Chen, L.; Zhao, Y. Neutrophil-to-lymphocyte Ratio as an Independent Risk Factor for Mortality in Hospitalized Patients with COVID-19. *J. Infect.* **2020**, *81* (1), No. E6−E12.
(38) Linghu, D.; Zhu, Z.; Zhang, D.; Luo, Y.; Ma, J.; Li, T.; Sun, Z.; Xie, Z.; Sun, J.; Cao, C. Diethylhexyl Phthalate Induces Immune Dysregulation and is an Environmental Immune Disruptor. *J. Hazard. Mater.* **2024**, *480*, 136244.
(39) Korniluk, A.; Koper-Lenkiewicz, O. M.; Kamińska, J.; Kemona, H.; Dymicka-Piekarska, V. Mean Platelet Volume (MPV): New Perspectives for an Old Marker in the Course and Prognosis of Inflammatory Conditions. *Mediators Inflamm.* **2019**, *2019*, 9213074.
(40) Passarella, S.; Schurr, A.; Portincasa, P. Mitochondrial Transport in Glycolysis and Gluconeogenesis: Achievements and Perspectives. *Int. J. Mol. Sci.* **2021**, *22* (23), 12620.
(41) Zhou, Y.; Khan, H.; Xiao, J.; Cheang, W. S. Effects of Arachidonic Acid Metabolites on Cardiovascular Health and Disease. *Int. J. Mol. Sci.* **2021**, *22* (21), 12029.
(42) Zhang, J.; Kong, X.; Zhou, C.; Li, L.; Nie, G.; Li, X. Toll-like Receptor Recognition of Bacteria in Fish: Ligand Specificity and Signal Pathways. *Fish Shellfish Immunol.* **2014**, *41* (2), 380−388.
(43) Lawrence, T. The Nuclear Factor NF-kappaB Pathway in Inflammation. *Cold Spring Harbor Perspect. Biol.* **2009**, *1* (6), a001651.
(44) Harjula, S. E.; Ojanen, M. J. T.; Taavitsainen, S.; Nykter, M.; Rämet, M. Interleukin 10 Mutant Zebrafish Have an Enhanced Interferon Gamma Response and Improved Survival Against a *Mycobacterium marinum* Infection. *Sci. Rep.* **2018**, *8* (1), 10360.
(45) Chen, D.; Zhang, Z.; Yao, H.; Cao, Y.; Xing, H.; Xu, S. Pro- and Anti-inflammatory Cytokine Expression in Immune Organs of the Common Carp Exposed to Atrazine and Chlorpyrifos. *Pestic. Biochem. Physiol.* **2014**, *114*, 8−15.
(46) Liu, Y.; Yin, H.; Zhao, M.; Lu, Q. TLR2 and TLR4 in Autoimmune Diseases: A Comprehensive Review. *Clin. Rev. Allergy Immunol.* **2014**, *47* (2), 136−147.
(47) Vallabhapurapu, S.; Karin, M. Regulation and Function of NF-kappa B Transcription Factors in the Immune System. *Annu. Rev. Immunol.* **2009**, *27*, 693−733.
(48) Kawahara, K.; Hohjoh, H.; Inazumi, T.; Tsuchiya, S.; Sugimoto, Y. Prostaglandin E2-induced Inflammation: Relevance of Prostaglandin E Receptors. *Biochim. Biophys. Acta* **2015**, *1851* (4), 414−421.
(49) Bryson, T. D.; Harding, P. Prostaglandin E2 EP Receptors in Cardiovascular Disease: An Update. *Biochem. Pharmacol.* **2022**, *195*, 114858.
(50) Fitzpatrick, F. A.; Lepley, R.; Orning, L.; Duffin, K. Effects of Leukotriene A4 on Neutrophil Activation. *Ann. N.Y. Acad. Sci.* **1994**, *714*, 64−74.